European Radiology (2020) 30:4772–4782
https://doi.org/10.1007/s00330-020-06867-w

HEPATOBILIARY-PANCREAS

Comparison between neuroendocrine carcinomas and well-differentiated neuroendocrine tumors of the pancreas using dynamic enhanced CT

Hyo Jung Park[1] · Hyoung Jung Kim[1] · Kyung Won Kim[1] · So Yeon Kim[1] · Sang Hyun Choi[1] · Myung-Won You[2] · Hee Sang Hwang[3] · Seung-Mo Hong[3]

Received: 15 January 2020 / Revised: 13 March 2020 / Accepted: 6 April 2020 / Published online: 28 April 2020

Abstract

Objectives To identify CT features distinguishing neuroendocrine carcinomas (NECs) of pancreas from well-differentiated neuroendocrine tumors (NETs) according to the World Health Organization 2017 and 2019 classification systems.

Methods This retrospective study included 69 patients with pathologically confirmed pancreatic neuroendocrine neoplasms who underwent dynamic CT (17, 17, 18, and 17 patients for well-differentiated grade 1, 2, 3 NET and NEC, respectively). CT was used to perform qualitative analysis (component, homogeneity, calcification, peripancreatic infiltration, main pancreatic ductal dilatation, bile duct dilatation, intraductal extension, and vascular invasion) and quantitative analysis (interface between tumor and parenchyma [delta], arterial enhancement ratio [AER], portal enhancement ratio [PER], and dynamic enhancement pattern). Uni- and multivariate logistic regression analyses were performed to identify features indicating NEC. Optimal cutoff values for enhancement ratios were determined.

Results NECs demonstrated significantly higher frequencies of main pancreatic ductal dilatation, bile duct dilatation, vascular invasion, and significantly lower delta (i.e., lower conspicuity), AER, and PER than well-differentiated NET ($p < 0.05$). On multivariate analysis, PER was the only independent factor selected by the model for differentiation of NEC from well-differentiated NET (odds ratio, < 0.001; 95% confidence interval [CI], < 0.001–0.012). PER < 0.8 showed the sensitivity of 94.1% (95% CI, 71.3–99.9) and the specificity of 88.5% (95% CI, 76.6–95.6). When three significant CT features were combined, the sensitivity and specificity for diagnosing NEC were 88.2% and 88.5%, respectively.

Conclusions Tumor-parenchyma enhancement ratio in portal phase is a useful CT feature to distinguish NECs from well-differentiated NETs. Combining qualitative and quantitative CT features may aid in achieving good diagnostic accuracy in the differentiation between NEC and well-differentiated NET.

Key Points

- *Neuroendocrine carcinoma of the pancreas should be distinguished from well-differentiated neuroendocrine tumor in line with the revised grading and staging system.*
- *Neuroendocrine carcinoma of the pancreas can be differentiated from well-differentiated neuroendocrine tumor on dynamic CT based on assessment of the portal enhancement ratio, arterial enhancement ratio, tumor conspicuity, dilatation of the main pancreatic duct or bile duct, and vascular invasion.*
- *Tumor-parenchyma enhancement ratio in portal phase of dynamic CT is a useful feature, which may help to distinguish neuroendocrine carcinoma from well-differentiated neuroendocrine tumor of the pancreas.*

Electronic supplementary material The online version of this article (https://doi.org/10.1007/s00330-020-06867-w) contains supplementary material, which is available to authorized users.

✉ Hyoung Jung Kim
hjk@amc.seoul.kr

[1] Department of Radiology and Research Institute of Radiology, Asan Medical Center, University of Ulsan College of Medicine, 88 Olympic-ro 43-gil, Songpa-gu, Seoul 05505, Republic of Korea

[2] Department of Radiology, Kyung Hee University Hospital, Seoul, Republic of Korea

[3] Department of Pathology, Asan Medical Center, University of Ulsan College of Medicine, Seoul, Republic of Korea

Keywords Pancreas · Carcinoma · Neuroendocrine · Neuroendocrine tumors · Multidetector computed tomography

Abbreviations

AER	Arterial enhancement ratio
G1	Grade 1
G2	Grade 2
G3	Grade 3
HU	Hounsfield unit
NEC	Neuroendocrine carcinoma
NET	Neuroendocrine tumor
PanNEN	Pancreatic neuroendocrine neoplasm
PD	Poorly differentiated
PER	Portal enhancement ratio
ROC	Receiver operating characteristics
ROI	Region of interest
WD	Well differentiated
WHO	World Health Organization

Introduction

Pancreatic neuroendocrine neoplasms (PanNENs) are a diverse group of tumors with heterogeneous clinical and biological features [1]. Recently, there have been rapid advances in our understanding of the pathophysiology and molecular biology of PanNEN, which have led to improvements in its diagnosis and treatment [2, 3]. In 2017, grading and staging for PanNEN changed considerably. In the WHO 2010 classification system, PanNENs were graded according to only the mitotic rate and/or Ki-67 index, and grade 3 (G3) tumors incorporated both well-differentiated (WD) tumors and poorly differentiated (PD) tumors [4]. However, since 2010, it has been recognized that some G3 tumors are histologically bland with WD histological pattern, show similar hormonal and genetic features as those of neuroendocrine tumors (NETs) [5, 6], and are less aggressive than other G3 tumors [7, 8]. In addition, some G3 tumors with Ki-67 index < 55% showed lower response but were associated with better survival than those with Ki-67 index > 55% after 1st-line platinum-based chemotherapy as that is used for PD neuroendocrine carcinomas (NECs) [9]. Considering this, the revised WHO 2017 system [10] classified PanNEN as G1, G2, and G3 NET (previously NEC with WD) and NEC, and the treatment strategies for NEC and WD G1/2/3 NET were also explicitly separated. Additionally, the WHO 2019 system expanded the WHO 2017 system from PanNEN to all NENs of the digestive tract [11], and the 8th edition of the American Joint Committee on Cancer (AJCC) staging manual separated the TNM staging system for NEC from WD G1/2/3 NET of the pancreas in that NEC follows staging system of exocrine tumors of the pancreas while WD G1/2/3 NET follows staging system of neuroendocrine tumors of the pancreas [12].

Therefore, for diagnosis and treatment planning, it is imperative to differentiate NEC from WD G1/2/3 NET. Previous studies have reported that G3 PanNENs have different CT characteristics from G1/2 tumors; G3 tumors are less enhanced and have more invasive features, including pancreatic or bile duct dilatation, or vascular invasion [13–15]. However, no studies have investigated the imaging features differentiating NEC from WD G1/2/3 NET, using the revised WHO 2017 system. Presence of a characteristic imaging feature suggestive of NEC may substantially aid in deciding the optimal diagnostic and treatment strategy for the patients. We aimed to identify the imaging features that differentiate NEC of the pancreas from WD G1/2/3 NET.

Materials and methods

This study was approved by our institution's institutional review board. The requirement for written informed consent was waived for this retrospective analysis.

Study population

We consecutively and retrospectively registered patients with pathologically confirmed PanNEN in our institution, a tertiary referral center, between January 2004 and January 2019. The following inclusion criteria were used: (a) patients who underwent surgery for WD G1/2 NET of the pancreas, or surgery or biopsy for WD G3 NET or NEC (please see "Pathology analysis" below); (b) patients who underwent dynamic enhanced CT scan within 30 days prior to surgery or biopsy; and (c) patients who did not receive local treatment or systemic therapy prior to the CT scan. Exclusion criteria were as follows: (a) pathology slide not adequate or available for review; and (b) PanNEN not visible on CT images. We identified 438 eligible patients (279 patients for WD G1 NET, 124 patients for WD G2 NET, 18 patients for WD G3 NET, and 17 patients for NEC, respectively). Patients with WD G1 and G2 NET were respectively matched one-to-one with the patients with NEC according to age, sex, and tumor size. The patient recruitment process is depicted in Fig. 1. The average time interval between CT scan and pathologic diagnosis was 7 days (range, 0–29 days).

Pathology analysis

Considering that pathologic analysis of PanNEN with a limited specimen obtained by fine-needle aspiration cytology or biopsy may underestimate the grade of the entire tumor due to heterogeneity within the tumor (for example, G3 tumors may

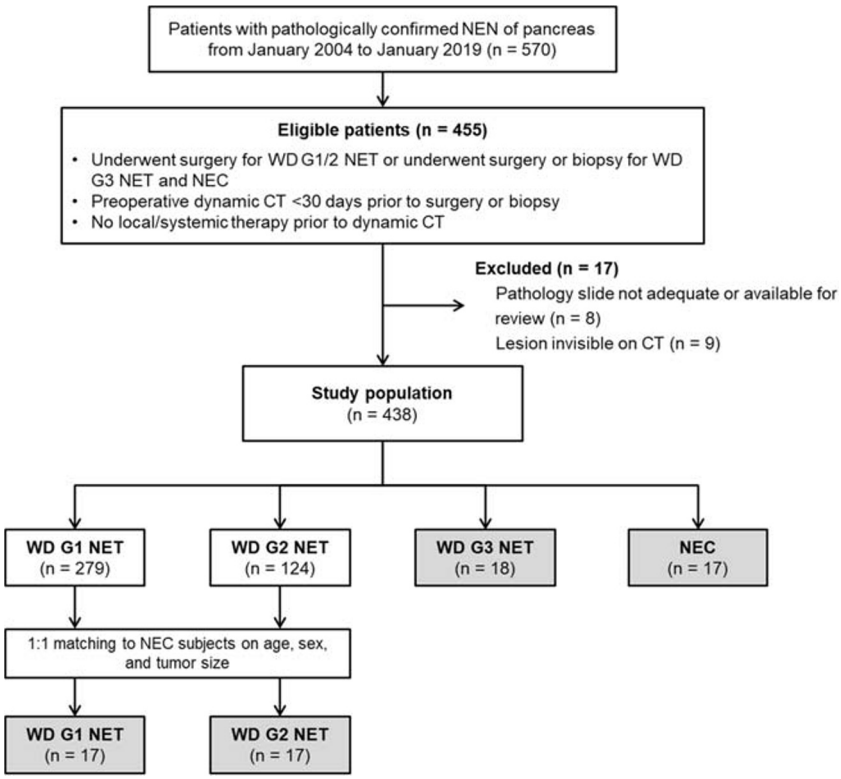

Fig. 1 Flow diagram of the patient recruitment process. NEN neuroendocrine neoplasm, NET neuroendocrine tumor, NEC neuroendocrine carcinoma, WD well-differentiated, G1 grade 1, G2 grade 2, G3, grade 3

be underestimated as G1 or G2 tumors by limited specimen analysis) [16], for WD G1/2 NET, we only included surgical resection cases. For WD G3 NET and NEC, we included surgical resection or biopsy cases for which the AJCC guidelines [12], particularly, a minimum of 50 high power fields (HPF) for the mitotic cell count and 500 cells for the Ki-67 index, were used for selection of biopsy specimens. One experienced pathologist (H.S.H, with 7 years of clinical experience in gastrointestinal pathology) reviewed all available pathology slides of PanNEN. Tumors were classified as WD G1 NET (< 2 mitoses per 10 HPFs and Ki-67 index, < 3%), WD G2 NET (2–20 mitoses per 10 HPF or Ki-67 index, 3–20%), WD G3 NET (> 20 mitoses per 10 HPF or Ki-67 index > 20%), and NEC (> 20 mitoses per 10 HPF or Ki-67 index > 20%) according to the revised 2017 WHO classification [10]. NECs were further classified as small cell type and large cell type according to the WHO 2019 classification [11].

Image techniques

The CT data were collected over a long period, using several CT techniques (Supplementary Table 1). CT images were obtained by using 16 or higher multidetector row systems. Dynamic CT images included non-enhanced, arterial, and portal venous phase images obtained for all patients. For contrast enhancement, the total volume of non-ionic iodinated contrast medium was stratified according to each patient's body weight (approximate rate, 2 mL/kg; maximum 150 mL), and an automatic power injector was used to deliver the agent intravenously (3 mL/s). Arterial phase images were obtained using a 10–15 s delay after aortic attenuation had reached 100 Hounsfield units (HUs). Portal venous phase images were obtained by using a fixed 75 s delay. CT images were acquired at 120 kVp and reconstructed with a 2.5–3 mm section thickness.

Image analysis

Qualitative analysis

CT images were anonymized and retrospectively reviewed by two board-certified abdominal radiologists (H.J.P. and K.W.K, with 6 and 12 years of experience in abdominal radiology, respectively) with consensus, using a picture archiving and communication system. The reviewers were aware of the presence of PanNEN but were blinded to the grade or differentiation. Disagreement between the two reviewers was minor and resolved by discussion. Items of qualitative analysis were as follows: (a) component, (b) homogeneity, (c) calcification, (d) peripancreatic infiltration, (e) main pancreatic ductal dilatation, (f) bile duct dilatation, (g) intraductal extension, and (h) vascular invasion. The tumor component was categorized as solid, solid and cystic, and complex cystic; each category indicated an enhancing solid portion of > 90%, 50–90%, < 50% of the tumor, respectively [14]. Tumor homogeneity was assessed on portal phase images and was categorized as

homogeneous or heterogeneous [17]. The presence of calcification within the tumor was evaluated via non-enhanced CT [14]. Main pancreatic ductal dilatation was defined if the diameter of main pancreatic duct distal to the tumor was 4 mm or greater [14]. Bile duct dilatation was defined as dilatation of both the extrahepatic (> 8 mm) and intrahepatic bile ducts (> 2 mm) [18]. Intraductal extension was defined as the tumor expanding into the adjacent main pancreatic duct, forming a voluminous intraductal soft tissue. The criteria for vascular invasion were more than 180° of tumor-vessel contact, irregularity of the vessel contour or change in caliber, tumor thrombus, or vessel occlusion [19].

Quantitative assessment

Items for quantitative assessment were as follows: (a) interface between tumor and parenchyma (delta), (b) arterial enhancement ratio (AER), (c) portal enhancement ratio (PER), and (d) dynamic enhancement pattern. Tumor conspicuity was quantitatively evaluated by analyzing the interface between tumor and surrounding pancreatic parenchyma by contouring region of interests (ROIs) at both the tumor and parenchyma at the border, and the mean value of HU distribution with each contour was subtracted, providing a difference in HU called "delta" [20]. The HU value of the tumor and parenchyma measured on arterial and portal phase images was recorded. HU values were determined by manually drawing a ROI within the tumor and the parenchyma on each phase CT. A radiologist drew the tumor-bearing ROI and parenchyma-bearing ROI as large as possible. We attempted to place the ROI in an identical site for each phase of CT in each patient. AER was calculated by dividing tumor HU value by parenchyma HU value that were measured on arterial phase images, and PER was measured by dividing tumor HU value by parenchyma HU value that were measured on portal venous phase images [14]. The dynamic enhancement pattern was categorized as early enhancement and washout (i.e., peak attenuation observed at the arterial phase and then decreased attenuation of more than 10 HU observed in the portal venous phase) [21], persistent enhancement (i.e., difference between attenuation on the arterial and portal venous phases of less than 10 HU), and progressive enhancement (i.e., peak attenuation observed at the portal venous phase with difference of attenuation between the arterial and portal venous phase of at least 10 HU).

Statistical analysis

The baseline characteristics of patients with WD G3 NET and NEC were compared using the independent *t* test, Fisher exact test, or χ^2 test depending on the type of data. CT imaging characteristics were compared between WD G1/2/3 NET and NEC using the independent *t* test, Fisher exact test, or χ^2 test as appropriate. Binary logistic regression analysis with forward projection method was performed to determine independent CT features that distinguish NEC from G1/2/3 NET, and their differential performance was evaluated using receiver operating characteristic (ROC) analysis with sensitivity and specificity of each cutoff value. In addition, the sensitivity and specificity of different combinations of the significant CT features were calculated to differentiate NEC from WD G1/2/3 NET. Each value of sensitivity and specificity was calculated using the number of significant CT findings as the cutoff point. We applied the same methods to compare CT imaging characteristics between WD G3 NET and NEC. Statistical significance was defined by a p value < 0.05. All statistical analyses were performed with SPSS software (version 21.0, IBM Corp).

Results

Characteristics of study population

We included 69 PanNENs patients (mean age, 55.1 ± 10.7 years; 47 men and 22 women), among whom 59 patients underwent surgery (85.5%), and 10 underwent biopsy only (14.5%). The tumor was located in the body or tail of the pancreas in 40 patients (58.0%), and in the head of the pancreas in 29 (42.0%). Among NECs, nine NECs were small cell type, seven NECs were large cell type, and one NEC was a combination of small cell and large cell carcinoma. The clinical characteristics of the study population are summarized in Table 1. There were no significant differences in age, sex, and tumor location between WD G3 NET and NEC (p = 0.827, 0.725 and 0.738, respectively).

Comparison of CT features between WD G1/2/3 NET and NEC

The summary of CT characteristics of WD G1/2/3 NET and NEC is shown in Table 2. Main pancreatic ductal dilatation and bile duct dilatation were significantly more frequent in NEC than WD G1/2/3 NET (82.4% [14/17] versus 26.9% [14/52] for main pancreatic ductal dilatation, respectively [p = 0.022], and 29.4% [5/17] versus 7.7% [4/52] for bile duct dilatation, respectively [p = 0.035]). Additionally, NEC had a significantly more frequent vascular invasion than WD G1/2/3 NET (64.7% [11/17] versus 26.9% [14/52], respectively, p = 0.008). There was a significant difference of delta between WD G1/2/3 NET (30.5 ± 20.5) and NEC (19.6 ± 11.2, p = 0.047, Fig. 2). Therefore, NEC had a significantly lesser tumor conspicuity than WD G1/2/3 NET. Regarding tumor-parenchyma enhancement ratio, the AER of NEC was significantly lower than that of WD G1/2/3 NET (0.6 ± 0.1 versus 1.1 ± 0.4, p < 0.001). The PER was also significantly lower in NEC than that of WD G1/2/3 NET (0.6 ± 0.2 versus 1.2 ± 0.3,

Table 1 Demographic characteristics of patients with WD G1/2/3 NET and NEC

Characteristics	WD NET ($n = 52$)			NEC ($n = 17$)	p value*
	G1 ($n = 17$)	G2 ($n = 17$)	G3 ($n = 18$)		
Age (year)†	53.8 ± 10.0	54.6 ± 12.1	55.5 ± 10.3	56.3 ± 11.0	0.827
Sex‡					0.725
Male	12 (70.6)	12 (70.6)	11 (61.1)	12 (70.6)	
Female	5 (29.4)	5 (29.4)	7 (38.9)	5 (29.4)	
Pathologic confirmation‡					0.146
Surgery	17 (100.0)	17 (100.0)	15 (83.3)	10 (58.8)	
Biopsy	0 (0.0)	0 (0.0)	3 (16.7)	7 (41.2)	
Tumor‡					
Location					0.738
Head	7 (41.2)	7 (41.2)	7 (38.9)	8 (47.1)	
Body or tail	10 (58.8)	10 (58.8)	11 (61.1)	9 (52.9)	
Size (mm) †	49.7 ± 22.3	51.7 ± 24.5	47.0 ± 36.6	56.2 ± 30.1	0.472
Stage‡§					0.560
I	1 (5.9)	1 (5.9)	0 (0.0)	1 (5.9)	
II	14 (82.4)	10 (58.8)	6 (33.3)	4 (23.5)	
III	2 (11.8)	2 (11.8)	6 (33.3)	4 (23.5)	
IV	0 (0.0)	4 (23.5)	6 (33.3)	8 (47.1)	

WD well-differentiated, *NET* neuroendocrine tumor, *NEC* neuroendocrine carcinoma

* p values were calculated from the comparison of grade 3 NET and grade 3 NEC

† Data are mean ± standard deviation. p values were calculated from student t test

‡ Data are number of patients with the percentage in parenthesis. p values were calculated from Fisher's test or χ^2 test

§ Based on American Joint Committee on Cancer Staging Manual 8th edition

$p < 0.001$). Therefore, in both arterial and portal phase images, NEC showed significantly lesser relative enhancement than WD G1/2/3 NET. Regarding the dynamic enhancement pattern, WD G1/2/3 NET had more frequent early enhancement and washout pattern than NEC while NEC demonstrated a higher frequency of persistent and progressive enhancement pattern without statistical significance ($p = 0.143$).

Table 2 CT features of WD G1/2/3 NET and NEC

Characteristics	WD G1/2/3 NET ($n = 52$)	NEC ($n = 17$)	Univariate p value	Multivariate Adjusted odds ratio‡	p value
Component*			> 0.999		
Solid	37 (71.2)	12 (70.6)			
Solid and cystic	15 (28.8)	5 (29.4)			
Homogeneity*			0.155		
Homogeneous	24 (46.2)	4 (23.5)			
Heterogeneous	28 (53.8)	13 (76.5)			
Calcification*	7 (13.5)	1 (5.9)	0.669		
Peripancreatic infiltration*	3 (5.8)	3 (17.6)	0.154		
Main pancreatic ductal dilatation*	14 (26.9)	14 (82.4)	0.022		
Bile duct dilatation*	4 (7.7)	5 (29.4)	0.035		
Intraductal extension*	5 (9.6)	1 (5.9)	> 0.999		
Vascular invasion*	14 (26.9)	11 (64.7)	0.008		
Delta†	30.5 ± 20.5	19.6 ± 11.2	0.047		
Arterial enhancement ratio†	1.1 ± 0.4	0.6 ± 0.1	< 0.001		
Portal enhancement ratio†	1.2 ± 0.3	0.6 ± 0.2	< 0.001	< 0.001 (< 0.001–0.012)	< 0.001
Dynamic enhancement pattern*			0.143		
Early enhancement and washout	10 (19.2)	0 (0.0)			
Persistent enhancement	11 (21.2)	5 (29.4)			
Progressive enhancement	31 (59.6)	12 (70.6)			

WD well-differentiated, *NET* neuroendocrine tumor, *NEC* neuroendocrine carcinoma

* Data are number of patients with the percentage in parenthesis. p values were calculated from Fisher's test or χ^2 test

† Data are mean ± standard deviation. p values were calculated from student t test

‡ Data are the odds ratio with 95% confidence interval in parenthesis

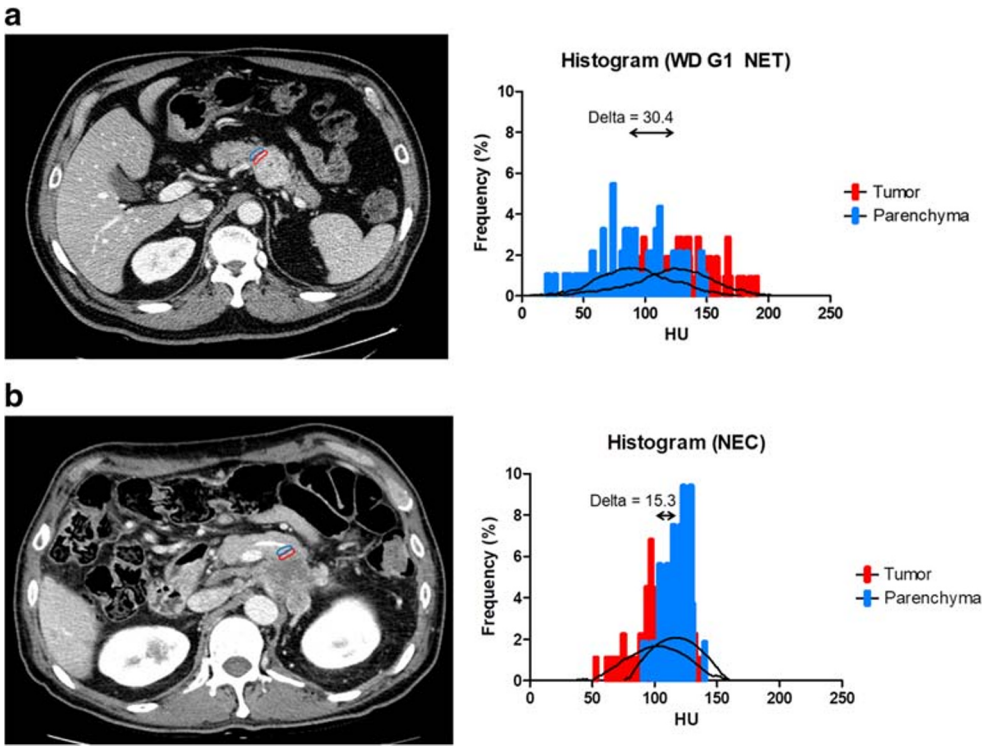

Fig. 2 Delta according to tumor grade and the corresponding HU histogram. ROI of the tumor and adjacent parenchyma at border is denoted by the blue and red line, respectively. **a** A WD G1 NET in a 65-year-old man. An axial portal venous phase CT image shows a 3.6-cm hyper-attenuated mass in the junction of pancreatic body and tail. There is a distinct margin between the tumor and the adjacent parenchyma. Delta is 30.4. **b** A NEC in a 55-year old man. In the axial portal venous phase CT image, there is a 5.2-cm hypo-attenuated mass with a poorly defined margin in the pancreatic tail. Delta is 15.3. HU Hounsfield unit, PanNEN pancreatic neuroendocrine neoplasm, ROI region of interest, WD well-differentiated, G1 grade 1, NET neuroendocrine tumor, NEC neuroendocrine carcinoma

After multivariate stepwise logistic regression analysis using variables with p value < 0.1 from univariate analysis (main pancreatic ductal dilatation, bile duct dilatation, vascular invasion, delta, AER, and PER), PER was the only independent factor selected by the model for differentiation of NEC from WD G1/2/3 NET ($p < 0.001$; adjusted odd ratio,

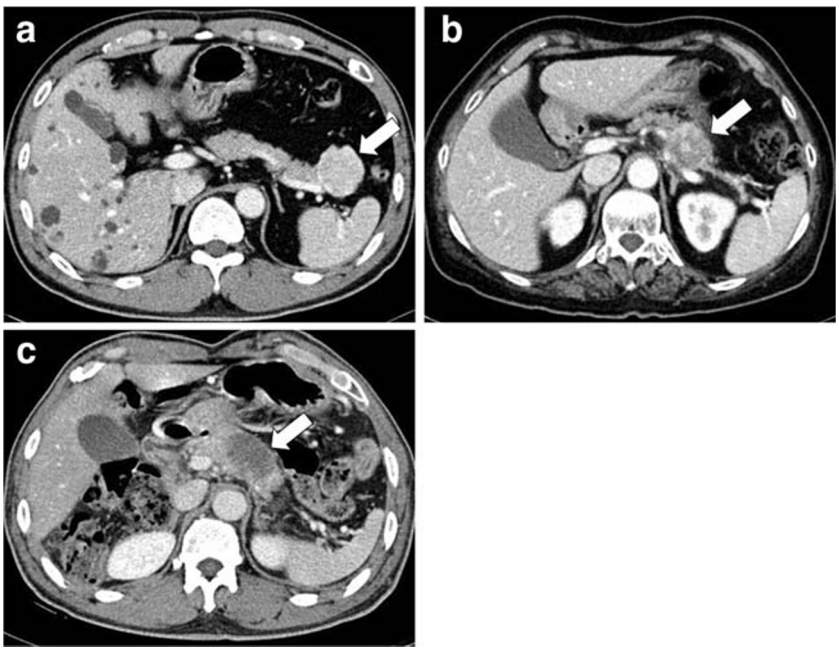

Fig. 3 PER of PanNEN according to tumor grade. **a** A WD G1 NET in a 55-year-old man. An axial portal venous phase CT image shows a 4.5-cm hyper-attenuated tumor (arrow) in the pancreatic tail. PER was 1.3. **b** A WD G3 NET in a 75-year-old woman. An axial portal venous phase CT image shows a 3.6-cm heterogeneously enhancing mass in the pancreatic tail (arrow). PER was 0.9. **c** An axial portal venous phase CT image of a 65-year-old man shows a 5.7-cm hypo-attenuated NEC in the pancreatic body (arrow), with PER of 0.5. PER portal enhancement ratio, PanNEN pancreatic neuroendocrine neoplasm, WD well-differentiated, G1 grade 1, NET neuroendocrine tumor, G3 grade 3, NEC neuroendocrine carcinoma

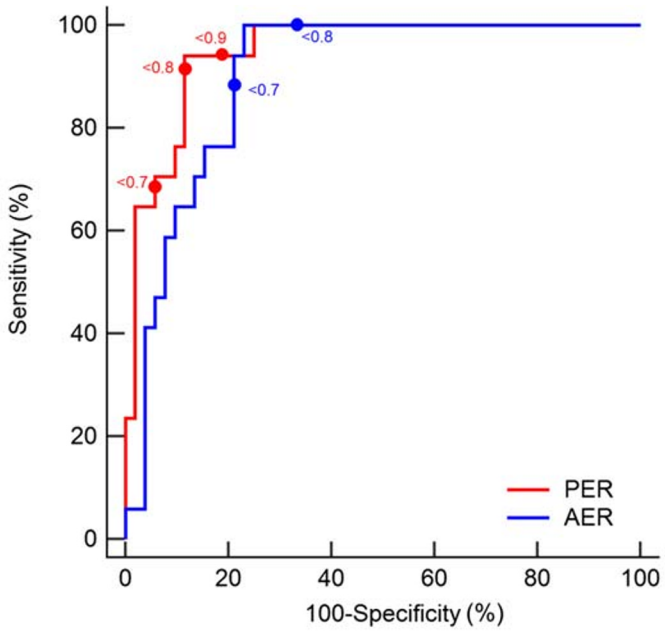

Fig. 4 The ROC curve, cutoff values, and corresponding sensitivity and specificity of each cutoff value of PER and AER for differentiating between NEC and G1/2/3 WD NET. The areas under the curve for PER and AER were 0.948 (95% CI, 0.866–0.987) and 0.900 (95% CI, 0.804–0.959), respectively. The sum of sensitivity and specificity was the highest for PER < 0.8. ROC receiver operating characteristic, PER portal enhancement ratio, AER arterial enhancement ratio, NEC neuroendocrine carcinoma, WD well-differentiated, NET neuroendocrine tumor, CI confidence intervals

	Sensitivity (%)	Specificity (%)	Odds ratio
PER			
<0.7	70.6 (44.0 – 89.7)	94.2 (84.1 – 98.8)	29.9 (6.5 – 138.6)
<0.8	94.1 (71.3 – 99.9)	88.5 (76.6 – 95.6)	57.5 (10.5 – 315.7)
<0.9	94.1 (71.3 – 99.9)	75.0 (61.1 – 86.0)	59.6 (7.1 – 500.4)
AER			
<0.7	94.1 (71.3 – 99.9)	78.9 (65.3 – 88.9)	17.4 (4.2 – 71.5)
<0.8	100.0 (80.5 – 100.0)	0.0 (0.0 – 6.8)	84.7 (4.8 – 1497.7)

< 0.001; 95% confidence interval [CI], < 0.001–0.012), with an area under the ROC curve of 0.948 (95% CI, 0.899–0.997). Figure 3 shows examples of PER of different grades of PanNEN.

A previous study used cutoff values of PER of < 0.9 and < 1.1 for differentiation of G1/2 tumors and G3 tumors [14]. Considering these threshold values and the mean values of PER of WD G1/2/3 NET and NEC of 1.2 and 0.6, respectively, we set the cutoff values as < 0.7, < 0.8, and < 0.9 and compared the performance of each value. Among them, PER < 0.8 showed the highest sum of sensitivity and specificity (sensitivity, 94.1%; specificity, 88.5%; odds ratio, 57.5; 95% CI, 10.5–315.7), and higher sum of sensitivity and specificity of the thresholds of AER (Fig. 4). Therefore, PER < 0.8 was selected as the variable in the evaluation of the sensitivity and specificity of CT findings (described below).

The sensitivity and specificity of each significant CT feature for differentiating WD G1/2/3 NET and NEC (main pancreatic ductal dilatation, bile duct dilatation, vascular invasion, delta, and PER) are summarized in Table 3. To determine the optimal threshold of delta, we compared the performance of delta < 20.0, < 25.0, and < 30.0; among them, delta < 25.0 was selected (sensitivity, 75.0%; specificity, 52.9%, odds ratio, 4.0; 95% CI, 1.1–13.9). The sensitivity and specificity of different combinations of CT features are shown in Table 4. When at least three of five CT features were used in combination, the sensitivity and specificity for diagnosing NEC were 88.2% and 88.5%, respectively.

Comparison of CT features between WD G3 NET and NEC

Table 5 shows the summary of CT characteristics of WD G3 NET and NEC. There was no qualitative parameter showing significant difference between WD G3 NET and NEC. Both demonstrated lesser enhancement than the adjacent normal parenchyma in the arterial and portal phase images. The AER and PER were both significantly lower in NEC than in WD G3 NET (0.6 ± 0.1 versus 0.8 ± 0.4 [$p = 0.011$], AER, and 0.6 ± 0.2 versus 0.9 ± 0.2 [$p < 0.001$], PER, respectively). Delta values were lower in NEC than WD G3 NET (19.6 ± 11.2 and 22.0 ± 14.4, respectively), but the difference was not significant ($p = 0.59$).

On multivariate regression analysis, tumor component, bile duct dilatation, AER, and PER were used as input variables. PER was the sole independent factor to differentiate NEC

Table 3 Sensitivity and specificity of each significant CT feature for differentiating between WD G1/2/3 NET and NEC

	Sensitivity (%)	Specificity (%)	Odds ratio
CT features			
Main pancreatic ductal dilatation	58.9 (32.9–81.6)	73.1 (59.0–84.4)	3.9 (1.2–12.2)
Bile duct dilatation	29.4 (10.3–56.0)	92.3 (81.5–97.9)	5.0 (1.2–21.5)
Vascular invasion	64.7 (38.3–85.8)	73.1 (59.0–84.4)	5.0 (1.5–16.0)
PER < 0.8	94.1 (71.3–99.9)	88.5 (76.6–95.6)	57.5 (10.5–315.7)
Delta < 25.0	75.0 (42.6–92.7)	56.9 (38.5–67.1)	4.0 (1.1–13.9)

WD well-differentiated, *NET* neuroendocrine tumor, *NEC* neuroendocrine carcinoma, *PER* portal enhancement ratio, *CI* confidence intervals

Data are values, with 95% confidence intervals in parentheses

from WD G3 NET ($p = 0.005$; adjusted odd ratio, < 0.001, 95% CI, < 0.001, 0.088, Fig. 3). The ROC analysis showed that the area under the curve of PER was 0.853 (95% CI, 0.726, 0.980). Among the cutoff values of < 0.7, < 0.8, and < 0.9, PER < 0.8 showed the highest sum of sensitivity and specificity (sensitivity, 94.1%; specificity, 66.7%; odds ratio, 15.0; 95% CI, 2.6–88.2) to differentiate between NEC and WD G3 NET. The sensitivity and specificity of each cutoff value of PER for differentiating NEC and WD G3 NET are shown in Fig. 5.

Discussion

The most compelling result of our study is that tumor-parenchyma enhancement ratio in portal phase (PER) was the independent factor to differentiate NEC from WD G1/2/3 NET of the pancreas. The mean PER of NEC and WD G1/2/3 NET was 0.6 and 1.2, respectively. PER could distinguish NEC from WD G3 NET (mean PER of 0.6 and 0.9 for NEC and WD G3 NET, respectively). To the best of our knowledge, this is the first study to compare imaging characteristics among the PanNEN grades according to the revised WHO 2017 and 2019 classification system [10, 11], in which G3 PanNENs were subdivided into WD G3 NET and NEC.

Prior studies based on WHO 2010 classification scheme showed that PER was distinct between lower and higher grade of PanNEN [14, 15, 22], supported by the histopathological analyses that suggested lesser tumor angiogenesis of higher grade PanNEN than lower grade [23]. Apart from the differences of grading in the previous classification system, previous studies reported that the degree of angiogenesis differed according to cell differentiation, based on the overall expression of angiogenic markers in WD NET as compared with that in NEC [24].

Delta, obtained by subtracting the mean HU of ROIs of tumor and parenchyma at the border, could be a useful and objective measure of tumor conspicuity. In Koay's study for pancreatic ductal adenocarcinoma, tumors with high delta (i.e., conspicuous tumors) were associated with more frequent distant metastasis and poorer prognosis; they were associated with lower frequency of stromal cell infiltration and more aggressive mutational and immunologic properties [20]. Poor prognosis in tumors with less stromal infiltration may be explained by that stromal portion may act to restrict metastatic spread of the cancer cells [25]. In PanNEN, the relationship between tumor conspicuity and prognosis appeared to be opposite of that in pancreatic ductal adenocarcinoma, because NEC showed significantly lower delta than WD G1/2/3 NET (mean value, 19.6 and 30.5, respectively). Previous studies have suggested that tumor conspicuity itself was associated with grade and prognosis of PanNEN [14, 15, 26] in that poorer tumor conspicuity suggested higher grade and poorer prognosis.

Table 4 Combinations of CT features for differentiating between WD G1/2/3 NET and NEC

Number of CT findings	Sensitivity (%)	Specificity (%)	Odds ratio
≥ 1	100.0 (80.5–100.0)	32.7 (20.3–47.1)	17.3 (0.9–304.0)
≥ 2	100.0 (80.5–100.0)	69.5 (49.0–76.4)	60.1 (3.4–1056.3)
≥ 3	88.2 (63.6–98.5)	88.5 (76.6–95.6)	57.5 (10.5–315.7)
≥ 4	17.7 (3.8–43.4)	100.0 (93.2–100.0)	25.3 (1.2–519.2)
≥ 5	5.9 (0.1–28.7)	100.0 (93.2–100.0)	9.5 (0.4–245.7)

WD well-differentiated, *NET* neuroendocrine tumor, *NEC* neuroendocrine carcinoma, *CI* confidence intervals

Data are values, with 95% confidence intervals in parenthesis

Includes main pancreatic ductal dilatation, bile duct dilatation, vascular invasion, PER < 0.8, and delta < 25.0

Table 5 CT features of WD G3 NET and NEC

Characteristics	WD G3 NET ($n = 18$)	NEC ($n = 17$)	Univariate p value	Multivariate Adjusted odds ratio‡	p value
Component*			0.088		
Solid	17 (94.4)	12 (70.6)			
Solid and cystic	1 (5.6)	5 (29.4)			
Homogeneity*			0.471		
Homogeneous	7 (38.9)	4 (23.5)			
Heterogeneous	11 (61.1)	13 (76.5)			
Calcification*	3 (16.7)	1 (5.9)	0.603		
Peripancreatic infiltration*	2 (11.1)	3 (17.6)	0.658		
Main pancreatic ductal dilatation*	7 (38.9)	14 (82.4)	0.318		
Bile duct dilatation*	1 (5.6)	5 (29.4)	0.088		
Intraductal extension*	2 (11.1)	1 (5.9)	> 0.999		
Vascular invasion*	8 (44.4)	11 (64.7)	0.315		
Delta†	22.0 ± 14.4	19.6 ± 11.2	0.590		
Arterial enhancement ratio†	0.8 ± 0.4	0.6 ± 0.1	0.011		
Portal enhancement ratio†	0.9 ± 0.2	0.6 ± 0.2	< 0.001	< 0.001 (< 0.001–0.008)	0.005
Dynamic enhancement pattern*			0.575		
Early enhancement and washout	1 (5.6)	0 (0.0)			
Persistent enhancement	6 (33.3)	5 (29.4)			
Progressive enhancement	11 (61.1)	12 (70.6)			

WD well-differentiated, *NET* neuroendocrine tumor, *NEC* neuroendocrine carcinoma

* Data are number of patients with the percentage in parenthesis. p values were calculated from Fisher's test or χ^2 test

† Data are mean ± standard deviation. p values were calculated from student t test

‡ Data are the odds ratio with 95% confidence interval in parenthesis

Main pancreatic ductal dilatation, bile duct dilatation, and vascular invasion were significantly more frequent, and AER was significantly lower in NEC than WD G1/2/3 NET. These features were all suggestive of higher grade of PanNEN from studies based on WHO 2010 classification [14, 15], and our study demonstrated these features are also possibly helpful for differentiating NEC from WD G1/2/3 NET according to the revised WHO classification.

The combination of qualitative and quantitative features showed high performance in differentiating WD G1/2/3 NET and NEC; number of CT findings ≥ 3 among main pancreatic ductal dilatation, bile duct dilatation, vascular invasion, PER < 0.8, and delta < 25.0 showed a sensitivity of 88.2% and specificity of 88.5% with odds ratio of 57.5 (95% CI, 10.5–315.7). Although PER was the only remaining independent indicator of NEC in multivariate analysis, combining qualitative and quantitative CT features may be helpful in achieving good diagnostic accuracy in the differentiation between NEC and WD G1/2/3 NET.

Overall, NEC and WD G3 NET showed fewer differences in imaging characteristics than NEC and WD G1/2/3 NET. The vascular invasion, main pancreatic ductal dilatation, and bile duct dilatation were significantly more frequent, and the AER and PER were significantly lower in NEC than WD G1/2/3 NET, which are parallel to the results of previous studies comparing lower and higher grade of PanNEN [14, 15, 17, 21, 22, 27]. Comparing NEC and WD G3 NET demonstrated significant differences in only AER and PER unlike other characteristics, with smaller differences in those two values than in comparison between NEC and WD G1/2/3 NET. For example, both NEC and WD G3 NET showed lesser enhancement than the adjacent normal parenchyma in both the arterial phase and portal phase images (i.e., in both groups, AER and PER were less than 1.0), whereas the mean value of AER and PER exceeded 1.0 in WD G1/2/3 NET. Since G3 PanNENs were all relatively aggressive tumors in the spectrum of PanNEN, the distinction of imaging characteristics may not be apparent between NEC and WD G3 NET compared with the distinction between NEC and WD G1/2/3 NET.

Recently, computer-assisted imaging analyses including histogram analysis, radiomics, and deep learning have gained attention for various imaging-based diagnostic and predictive tasks. Several attempts have been made to predict the grades of PanNEN using CT or MRI, particularly G1 tumors versus G2/3 tumors using histogram analysis and radiomics, with promising results [28, 29]. According to the revised grading system, future studies to differentiate WD NETs and NECs using these advanced techniques are anticipated.

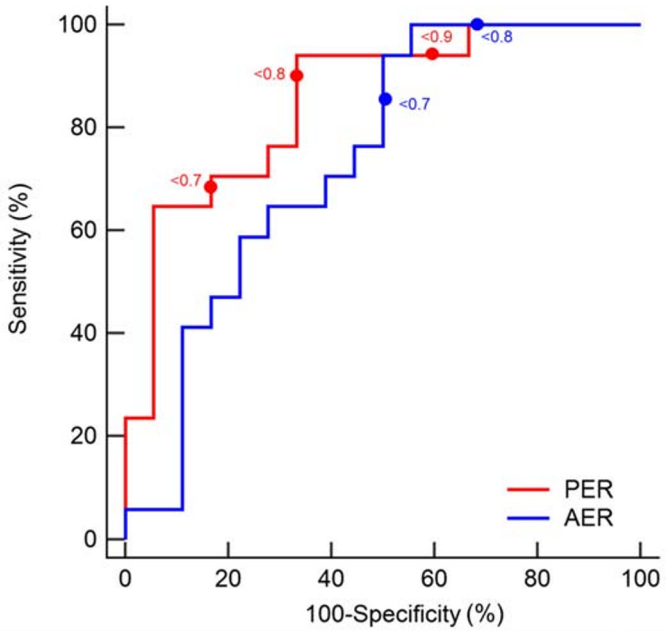

Fig. 5 The ROC curve, cutoff values, and corresponding sensitivity and specificity of each cutoff value of PER and AER for differentiating between NEC and G3 WD NET. The area under the curve for PER and AER were 0.853 (95% CI, 0.692–0.949) and 0.739 (95% CI, 0.563–0.872), respectively. The sum of sensitivity and specificity was the highest for PER < 0.8. ROC receiver operating characteristic, PER portal enhancement ratio, AER arterial enhancement ratio, NEC neuroendocrine carcinoma, WD well-differentiated, NET neuroendocrine tumor, CI confidence intervals

	Sensitivity (%)	Specificity (%)	Odds ratio
PER			
<0.7	70.6 (44.0 – 89.7)	83.3 (58.6 – 96.4)	9.2 (1.9 – 44.9)
<0.8	94.1 (71.3 – 99.9)	66.7 (41.0 – 86.7)	15.0 (2.6 – 88.2)
<0.9	94.1 (71.3 – 99.9)	33.3 (13.3 – 59.0)	12.8 (1.4 – 118.3)
AER			
<0.7	94.1 (71.3 – 99.9)	50.0 (26.0 – 74.0)	4.7 (0.9 – 22.0)
<0.8	100.0 (80.5 – 100.0)	0.0 (0.0 – 18.5)	18.2 (0.9 – 353.6)

Our study has several limitations. First, the retrospective study design from single institution may have introduced selection biases and small sample size. Due to the low incidence of PanNEN, particularly NEC, the study population was inevitably small. However, in comparison of imaging characteristics between tumor groups, we tried to minimize potential confounders by matching WD G1/2 NET with NEC with patients' age, sex, and tumor size. Second, because of the long patient recruitment period, various CT scanners were used, which might have affected the image analysis. Third, according to our institutional protocol for vascular assessment using dynamic CT scans, arterial phase images were acquired slightly before than usual pancreatic phase images, and this may have influenced AER assessment. Fourth, due to the unavoidable small study population, we could not validate our result in a separate dataset. However, our study includes the largest number of NECs among published studies to date for comparison between well-differentiated NETs and NECs. Further studies are highly anticipated to verify our study findings.

In conclusion, NEC of the pancreas can be differentiated from WD G1/2/3 NET and from WD G3 NET using dynamic CT. The tumor-parenchyma enhancement ratio in portal phase image is a useful CT feature which may help to differentiate NEC from WD G1/2/3 NET as well as from WD G3 NET of the pancreas. Combining qualitative and quantitative CT features may be helpful in achieving good diagnostic accuracy in the differentiation between NEC and WD G1/2/3 NET.

Acknowledgments Authors would like to express their appreciation to Dr. Yu Sub Sung for his assistance in measuring delta and making Fig. 2.

Funding information The authors state that this work has not received any funding.

Compliance with ethical standards

Guarantor The scientific guarantor of this publication is Hyoung Jung Kim.

Conflict of interest The authors of this manuscript declare no relationships with any companies whose products or services may be related to the subject matter of the article.

Statistics and biometry No complex statistical methods were necessary for this paper.

Informed consent Written informed consent was waived by the Institutional Review Board.

Ethical approval Institutional Review Board approval was obtained.

Study subjects or cohorts overlap Some study subjects or cohorts have been previously reported in:

a. Kim DW, Kim HJ, Kim KW, et al (2015) Neuroendocrine neoplasms of the pancreas at dynamic enhanced CT: comparison between grade 3 neuroendocrine carcinoma and grade 1/2 neuroendocrine tumour. Eur Radiol 25:1375–1383.

b. Kim JY, Kim MS, Kim KS, et al (2015) Clinicopathologic and prognostic significance of multiple hormone expression in pancreatic neuroendocrine tumours. Am J Surg Pathol 39:592–601.

c. Son EM, Kim JY, An S et al (2015) Clinical and prognostic significances of cytokeratin 19 and KIT expression in surgically resectable pancreatic neuroendocrine tumors. J Pathol Transl Med 49:30–36.

d. Hwang HS, Kim Y, An S et al (2018) Grading by the Ki-67 labeling index of endoscopic ultrasound-guided fine-needle aspiration biopsy specimens of pancreatic neuroendocrine tumors can be underestimated. Pancreas 47:1296–1303.

Methodology
- retrospective
- diagnostic or prognostic study
- performed at one institution

References

1. Singhi AD, Klimstra DS (2018) Well-differentiated pancreatic neuroendocrine tumours (PanNETs) and poorly differentiated pancreatic neuroendocrine carcinomas (PanNECs): concepts, issues and a practical diagnostic approach to high-grade (G3) cases. Histopathology 72:168–177
2. Lawrence B, Gustafsson BI, Chan A, Svejda B, Kidd M, Modlin IM (2011) The epidemiology of gastroenteropancreatic neuroendocrine tumors. Endocrinol Metab Clin North Am 40:1–18
3. Choe J, Kim KW, Kim HJ et al (2019) What is new in the 2017 World Health Organization classification and 8th American joint committee on cancer staging system for pancreatic neuroendocrine neoplasms? Korean J Radiol 20:5–17
4. Bosman FT, Carneiro F, Hruban RH, Theise ND (2010) WHO classification of tumours of the digestive system, 4th edn. International Agency for Research on Cancer, Lyon
5. Basturk O, Tang L, Hruban RH et al (2014) Poorly differentiated neuroendocrine carcinomas of the pancreas: a clinicopathologic analysis of 44 cases. Am J Surg Pathol 38:437–447
6. Yachida S, Vakiani E, White CM et al (2012) Small cell and large cell neuroendocrine carcinomas of the pancreas are genetically similar and distinct from well-differentiated pancreatic neuroendocrine tumors. Am J Surg Pathol 36:173–184
7. Basturk O, Yang Z, Tang LH et al (2015) The high-grade (WHO G3) pancreatic neuroendocrine tumor category is morphologically and biologically heterogenous and includes both well differentiated and poorly differentiated neoplasms. Am J Surg Pathol 39:683–690
8. Heetfeld M, Chougnet CN, Olsen IH et al (2015) Characteristics and treatment of patients with G3 gastroenteropancreatic neuroendocrine neoplasms. Endocr Relat Cancer 22:657–664
9. Sorbye H, Strosberg J, Baudin E, Klimstra DS, Yao JC (2014) Gastroenteropancreatic high-grade neuroendocrine carcinoma. Cancer 120:2814–2823
10. Lloyd RV, Osamura RY, Klöppel G et al (2017) WHO classification of tumours of endocrine organs, 4th edn. International Agency for Research on Cancer, Lyon
11. WHO Classification of Tumours Editorial Board (2019) Digestive system tumours, 5th edn. International Agency for Research on Cancer, Lyon
12. Amin MB, Edge SB, Greene FL, et al (2017) AJCC cancer staging manual, 8th edn. Springer, New York
13. Horiguchi S, Kato H, Shiraha H et al (2017) Dynamic computed tomography is useful for prediction of pathological grade in pancreatic neuroendocrine neoplasm. J Gastroenterol Hepatol 32:925–931
14. Kim DW, Kim HJ, Kim KW et al (2015) Neuroendocrine neoplasms of the pancreas at dynamic enhanced CT: comparison between grade 3 neuroendocrine carcinoma and grade 1/2 neuroendocrine tumour. Eur Radiol 25:1375–1383
15. D'Onofrio M, Ciaravino V, Cardobi N et al (2019) CT enhancement and 3D texture analysis of pancreatic neuroendocrine neoplasms. Sci Rep 9:2176
16. Hwang HS, Kim Y, An S et al (2018) Grading by the Ki-67 labeling index of endoscopic ultrasound-guided fine needle aspiration biopsy specimens of pancreatic neuroendocrine tumors can be underestimated. Pancreas 47:1296–1303
17. Canellas R, Burk KS, Parakh A, Sahani DV (2018) Prediction of pancreatic neuroendocrine tumor grade based on CT features and texture analysis. AJR Am J Roentgenol 210:341–346
18. Gore R, Levine M (2008) Textbook of gastrointestinal radiology. Saunders, Philadelphia
19. Al-Hawary MM, Francis IR, Chari ST et al (2014) Pancreatic ductal adenocarcinoma radiology reporting template: consensus statement of the Society of Abdominal Radiology and the American Pancreatic Association. Radiology 270:248–260
20. Koay EJ, Lee Y, Cristini V et al (2018) A visually apparent and quantifiable CT imaging feature identifies biophysical subtypes of pancreatic ductal adenocarcinoma. Clin Cancer Res 24:5883–5894
21. Belousova E, Karmazanovsky G, Kriger A et al (2017) Contrast-enhanced MDCT in patients with pancreatic neuroendocrine tumours: correlation with histological findings and diagnostic performance in differentiation between tumour grades. Clin Radiol 72:150–158
22. Guo C, Zhuge X, Wang Z et al (2019) Textural analysis on contrast-enhanced CT in pancreatic neuroendocrine neoplasms: association with WHO grade. Abdom Radiol (NY) 44:576–585
23. Marion-Audibert AM, Barel C, Gouysse G et al (2003) Low microvessel density is an unfavorable histoprognostic factor in pancreatic endocrine tumors. Gastroenterology 125:1094–1104
24. Couvelard A, O'Toole D, Turley H et al (2005) Microvascular density and hypoxia-inducible factor pathway in pancreatic endocrine tumours: negative correlation of microvascular density and VEGF expression with tumour progression. Br J Cancer 92:94–101
25. Rhim AD, Oberstein PE, Thomas DH et al (2014) Stromal elements act to restrain, rather than support, pancreatic ductal adenocarcinoma. Cancer Cell 25:735–747
26. Luo Y, Dong Z, Chen J et al (2014) Pancreatic neuroendocrine tumours: correlation between MSCT features and pathological classification. Eur Radiol 24:2945–2952
27. Takumi K, Fukukura Y, Higashi M et al (2015) Pancreatic neuroendocrine tumors: correlation between the contrast-enhanced computed tomography features and the pathological tumor grade. Eur J Radiol 84:1436–1443
28. De Robertis R, Maris B, Cardobi N et al (2018) Can histogram analysis of MR images predict aggressiveness in pancreatic neuroendocrine tumors? Eur Radiol 28:2582–2591
29. Gu D, Hu Y, Ding H et al (2019) CT radiomics may predict the grade of pancreatic neuroendocrine tumors: a multicenter study. Eur Radiol 29:6880–6890